High-quality Single-walled carbon nanotubes synthesis by hot filament CVD on Ru nanoparticule catalyst

Fatima Zara Bouanis, Laurent Baraton, Vincent Huc, Didier Pribat, Costel Sorin Cojocaru

Thin Solid Films
519 (2011) 4594–4597
DOI: http://dx.doi.org/10.1016/j.tsf.2011.01.326

High-quality single-walled carbon nanotubes synthesis by hot filament CVD on Ru nanoparticle catalyst

Fatima Z. Bouanis [a], Laurent Baraton [a], Vincent Huc [b], Didier Pribat [a], Costel S. Cojocaru [a,*]

[a] Laboratoire de physique des interfaces et couches minces UMR 7647 CNRS/ Ecole Polytechnique PALAISEAU, France
[b] Laboratoire de Chimie inorganique LCI-ICMMO UMR 8182 - Bât. 420 Université Paris-Sud 11 Orsay, France

a b s t r a c t

We investigated the single-walled carbon nanotubes (SWCNTs) growth on Ru nanoparticle catalyst via hot filament assisted chemical vapor deposition (HFCVD) with two independent W filaments for the carbon precursor (methane) and the hydrogen dissociation respectively. The Ru nanoparticles were obtained following a two-step strategy. At first the growth substrate is functionalized by silanisation, then a self assembly of a ruthenium porphyrin complex monolayer on pyridine-functionalized metal oxide substrates. We have studied the impact of the filaments power and we optimized the SWCNTs growth temperature. The as grown SWCNTs were characterized by scanning electron microscopy (SEM), atomic force microscopy (AFM) and Raman spectroscopy. It was found that the quality, density and the diameter of SWCNTs depends on the filament and growth temperature. Results of this study can be used to improve the understanding of the growth of SWCNTs by HFCVD.

Keywords:
Single walled carbon nanotubes (SWCNTs) Hot filament CVD
Self assembled monolayer
Ru nanoparticle
Raman spectroscopy

1. Introduction

Due to their unique mechanical, electrical and chemical properties [1], carbon nanotubes (CNTs), particularly single walled (SW) CNTs, represent exciting opportunities for fundamental science and new technologies [2]. Development and progress in the synthesis methods for large-scale production of single-walled carbon nanotubes (SWCNTs) over the past decade have paved the way for many potential applications as electronic nanodevices [3], electrical wiring [4], biodevices [5], probes for scanning probe microscopy [6], etc. The integration of CNTs into nano-electronic devices essentially requires the ability to control CNT growth in terms of diameter and chirality, since their electronic properties are determined by the nanotubes structure [1].

Among the variety of synthesis techniques for SWCNTs, the chemical vapor deposition (CVD) [1], in which a hydrocarbon is thermally decomposed over a metallic catalyst, is particularly attractive as it allows to selectively control the growth of CNTs with defined morphologies by adjusting reaction parameters such as carbon source, catalyst type, reaction temperature, and so on. More importantly, it is the most suitable method for industrial-scale production, because of its upward scalability and low cost. In addition to the "classical" thermal CVD, various CVD methods have been developed over time, including the plasma enhanced CVD (PECVD) and the hot-filament assisted CVD (HFCVD) [7,8]. The PECVD method presents many advantages such as control of the vertical alignment of nanotubes due to the intrinsic electric field of the plasma sheath [9,10] and low processing temperature (~500 °C). However, carbon nanotubes grown by PECVD are overwhelmingly carbon nanofibers (CNFs) or multi-walled carbon nanotubes (MWCNTs) with measurable structural defects. The synthesis of SWCNTs seems to be difficult by this method, due to the production of high order hydrocarbons and radicals in a plasma environment [11]. Depending on the final application, HFCVD could be even more desirable than plasma CVD because HFCVD processes are more economical and suitable for large-area and irregular-shaped substrates [7]. Thus, a large variety of substrates of any sizes and shapes compatible with the furnace dimensions, growth temperature, and gas environment can be coated with CNTs [12].

The aim of the present paper is to study the growth of SWCNTs via HFCVD with Ru as catalyst and CH_4 as a carbon source. The Ru catalyst was prepared in two steps: (i) the growth substrate is functionalized by silanisation, leading to the formation of a pyridine terminated molecular monolayer. (ii) self assembled monolayers (SAM) of metallic complexes such as Ru tetraphenyl porphyrins (RuTPP) are then obtained by coordination between the Ru ions and the pyridine groups pointing outwards the surface. The method allows to control the size and the surface density of the catalytic metallic nanoparticles formed through a subsequently annealing step. In conjunction with a proper selection of synthesis parameters this can further allow some control on the SWCNTs diameters, their surface density and eventually to a certain selectivity of their chirality [13,14].

2. Experimental

2.1. Catalyst preparation

The Ru containing self-assembled organic monolayer that serves as a catalyst precursor was synthesized in a two step process. In the first

step, a pyridine terminated monolayer is formed on an RCA (Radio Corporation of America) cleaned [15] silicon oxide substrate through a silanisation reaction. Full synthesis of the organosilane used for this step and the characterization of the monolayer will be detailed in a forthcoming paper [16]. Briefly, the silanisation reaction is carried out overnight in anhydrous toluene under argon flushing. Silanisation solution contained 100 mg of the organosilane for 100 ml of toluene. These pyridine-functionalized substrate is then used as an anchor of the second metallic complex containing layer. Porphyrin complexes are used for these experiments, as it is already demonstrated that these molecules are prone to self-assemble on surfaces as high quality monolayers [13,17]. In our study, we used an RuTTP complex (5,10,15,20-Tetraphenyl-21H,23H-porphine ruthenium(II) carbonyl - Sigma Aldrich - 1 mg/ml in anhydrous CH_2Cl_2). All chemicals were used as received.

2.2. Synthesis of carbon nanotubes (CNTs)

The homemade experimental HFCVD set-up system used to grow SWCNTs has been previously [18] described. Briefly it consists in a quartz tube enclosed in a cylindrical heater. It is connected to the methane and hydrogen feedstock and to a pumping system (residual base pressure 10^{-6} mbar). The methane and hydrogen are injected as separate flows and forced to pass over two separate tungsten filaments (0.38 mm in diameter), mounted horizontally near the substrate, and independently electrically driven at variable power. Thus this set-up can be used as a classical thermal CVD set-up or as a HFCVD one. Typical experimental conditions were as follows: after loading into the CVD system, once the working temperature is reached, the sample, sitting on a quartz boat, is introduced in the hot zone of the tube. Then the samples are pre-exposed to a hot-filament activated (160 W−approximately 1900 °C) hydrogen flow for 5 min at 90 mbar, in order to burn the organic monolayer and free the Ru catalyst. Subsequently the CNTs growth was performed for 30 min at variable growth temperature (800 °C to 1000 °C) with a CH_4 relative concentration of 10% and either by a classical CVD process or a HFCVD process. In the latter case, the CH_4 filament is heated up to 1700 °C using a 120 W filament power.

2.3. Characterization techniques

The morphologies of the CNTs on silicon oxide substrates were characterized by atomic force microscopy (AFM; Veeco 3100) and scanning electron microscopy (SEM; HITACHI S 4800). The carbon nanotubes quality was confirmed using a high-resolution confocal Raman microscope (Labram HR800; HORIBA Jobin Yvon) in the normal incident backscattering configuration, using the 100× objective. Excitation wavelength of 632.8 nm is provided by the built-in HeNe laser of the spectrometer. The incident laser power was less than 1 mW, collection time 5 s, with 2 accumulations.

3. Results and discussion

3.1. Catalyst

The thickness of the silane layer (SAM) measured by ellipsometry is 1.2 nm, in accordance with the length of the molecule. This result suggests that the molecules are standing upright on the surface. The quality of that molecular layer was also characterized by AFM, presented in [16].

The thickness of a SAM of a Ru porphyrin was evaluated by transmission UV-VIS spectroscopy on transparent glass slides. An absorbance peak centered at 418 nm and of an intensity of ~0.2 confirmed the formation of a single porphyrin overlayer on top of the pyridine terminated silane monolayer. This control experiment shows that the formation of high quality monolayers of metallic complexes on surfaces is easily obtained according to our self-assembly based approach.

3.2. Effect of hot filament

We first investigated the impact of the CH_4 pre-dissociation via the hot filament by comparison with carbon nanotubes samples grown without hot filament assistance. Previous reports [19,20], indicate that carbon radicals species resulting from the CH_4 catalytic decomposition over a hot filament can strongly enhance the formation of CNTs over the catalyst particles.

Fig. 1 resumes the Raman spectra recorded in the high frequency region (1000–2000 cm^{-1}) (a) and the low-frequency region (100–350 cm^{-1}) (b) of the two CNT films grown on Ru catalyst with and without hot filament assistance.

Raman spectroscopy is a powerful technique to identify and evaluate the quality of as-prepared SWCNTs products [11]. In the high frequency range (Fig. 1a) two main Raman features are observed. The D band at ~1310 cm^{-1}, originates from crystalline disorders and lattice defects in the curved graphene sheets [22–24]. The G band at ~1590 cm^{-1} corresponds to the high-frequency E_{2g} first-order mode of highly oriented pyrolytic graphite. The G band splits in two components (G^- and G^+). The G^- band at ~1585 cm^{-1}, which is due to the curvature of the tube [21], can generally only be discerned when the nanotube diameter is sufficiently small. Usually, the value of I_D/I_G (ratio of the areal intensities of the D-band and over the G-band) is used to evaluate the amount of disorder within carbonaceous materials and nanotubes in particular [25]. One can notice from Fig. 1a that the value of I_D/I_G decreases when hot filament is used (0.09 and 0.15 for samples growth with and without HF, respectively), indicating an increasing crystalline quality of the films. Also,

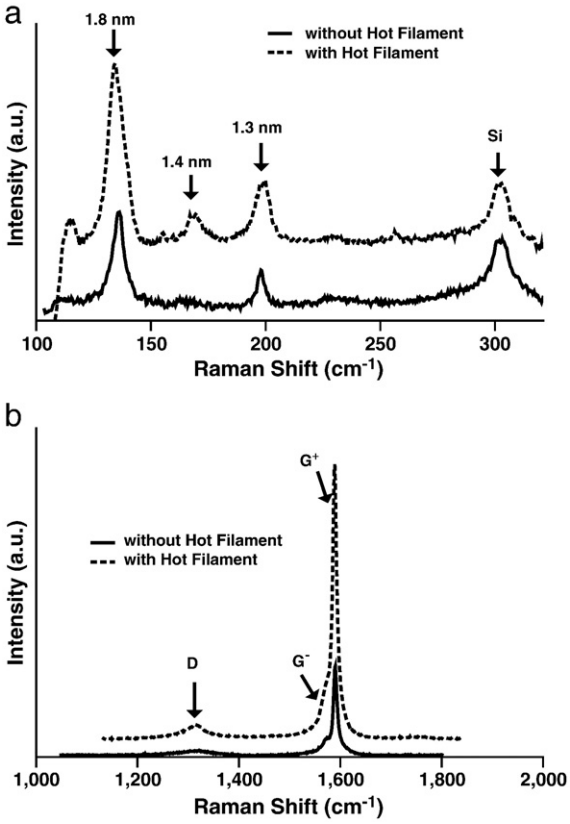

Fig. 1. (a and b) Raman spectra in high frequency region and low frequency region, respectively, for the samples growth with and without hot filament CVD. Growth parameters; growth temperature: 900 °C, CH_4 concentration: 10 sccm and growth time: 30 min.

from Fig. 1b, we notice that the Raman spectra of the samples grown without hot filament exhibit two main active radial breathing mode (RBMs), representing the A_{1g} symmetry mode [26], at 135 cm^{-1} and 197 cm^{-1} corresponding to SWCNTs diameters of 1.8 nm and 1.2 nm, respectively. The diameters of SWCNTs where calculated using $d_{SWCNTs} =$ [27], were d_{SWCNTs}[nm] is SWCNTs diameter and ω_{RBM} [cm^{-1}] the wavenumber of RBM [28,29]. By comparison (Fig. 1b), the overall RBM modes intensity is significantly increased for the sample prepared with hot filament assistance and also the number of RBM peaks increases. This trend is further confirmed by the SEM observations in Fig. 2 as they reveal that both the density and the length of SWCNTs increase when the hot filament is used.

These results indicate that high quality SWCNTs can be effectively grown with hot filament assistance. The CH_4 pre-decomposition into carbon radicals and hydrocarbon species when it passed through the filament leads to an increased concentration of reactive carbon species on the catalyst particles [10,30]. This may explain the higher yield of SWCNTS on the surface, the enhanced growth rate and the lower number of defaults of the resulting nanotubes.

3.3. Effect of temperature on growth of SWCNTs

The growth temperature is one of the most important parameter impacting the yield and the SWCNTs quality grown by classical "thermal" CVD methods. Figs. 3 and 4 summarize the Raman and respectively the SEM/AFM observations of the CNTs grown by HFCVD at different temperatures: 800 °C, 900 °C and 1000 °C while the CH_4 concentration and growth time were kept constant at 10% and 30 min, respectively. Both hot filaments were powered on as described above.

Fig. 3(a) and (b) shows the corresponding Raman spectra in the RBM frequency region and the high frequency region, respectively. One can notice the clear signatures of well-crystallized SWCNTs, namely a strong presence of radial breathing modes (RBM), a very small D-band (~1310 cm^{-1}) and an intense G-band (~1580 cm^{-1}) for both the samples grown at higher temperatures. We should also notice that by contrast with the sample grown at 900 °C exhibiting a very low I_D/I_G ratio (lower than 0.09), the sample grown at 1000 °C presents a higher I_D/I_G ratio of approximately 0.2. The Raman features for the sample grown at 800 °C are very weak and present an I_D/I_G intensity ratio near to unity.

As well, RBM peaks, characteristic of the SWCNTs, are observed only for the samples synthesized at temperatures of 900 °C and higher, suggesting a threshold temperature somewhere between 800 °C and 900 °C for SWCNTs synthesis under the chosen conditions. Typically, samples grown at 900 °C exhibit only three peaks at 139 cm^{-1}, 149 cm^{-1} and 193 cm^{-1}, corresponding to SWCNTs diameters of 1.78 nm, 1.66 nm and 1.28 nm respectively, indicating a narrow initial distribution of small diameter catalyst particles. For SWCNTs grown at 1000 °C, we observe only the intense RBM peak at 138 cm^{-1} and a much less intense peak shifted at 196 cm^{-1}. The shift of the less intense RBM from 193 cm^{-1} to 197 cm^{-1} when growth temperature is increased from 900 °C to 1000 °C, suggest that the synthesis of larger-diameter SWCNTs is preferred at higher temperature as previously observed and predicted [31,32]. The increase of the temperature allows easier diffusion of the catalyst atoms and particles on the growth substrate, thus leading to larger catalyst particles due to the higher collision probability that in turn, leads to larger diameters SWCNTs formation.

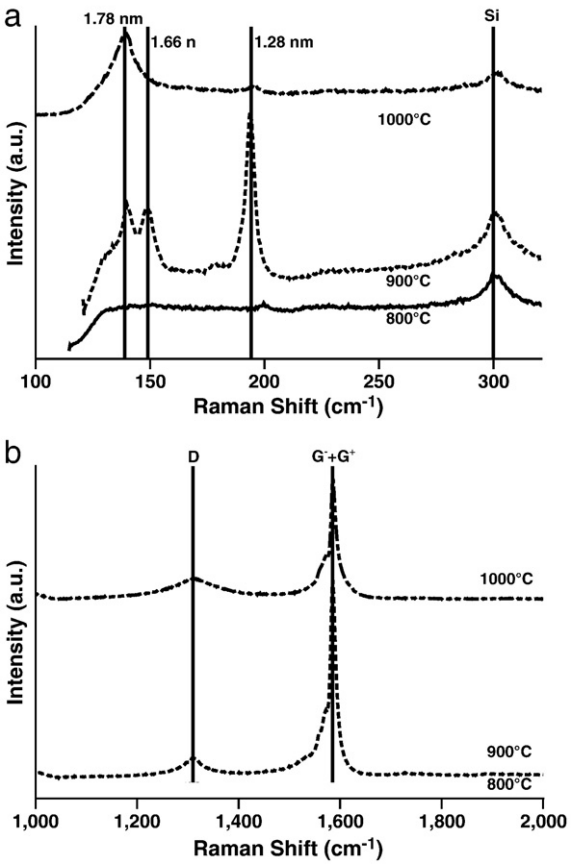

Fig. 3. (a and b) Raman spectra in high frequency region and RBM region, respectively, for the SWCNTs film deposited as a function of growth temperature. The growth condition was 30 min and 10 sccm. Si indicates Raman peak of the substrate at approximately 300 cm^{-1}.

These results are confirmed by the SEM and the AFM observations summarized in Fig. 4. No CNTs growth could be observed when the growth temperature was 800 °C probably related to the insufficient growth kinetic energy at lower growth temperature [33]. On the contrary, starting from 900 °C, quite dense carbon nanotubes could be observed on the substrate, as the nucleation and the growth of the

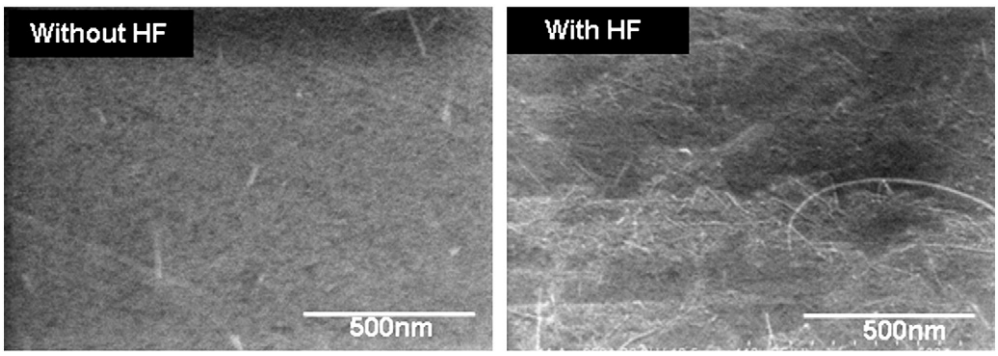

Fig. 2. SEM images for the samples growth with and without hot filament CVD.

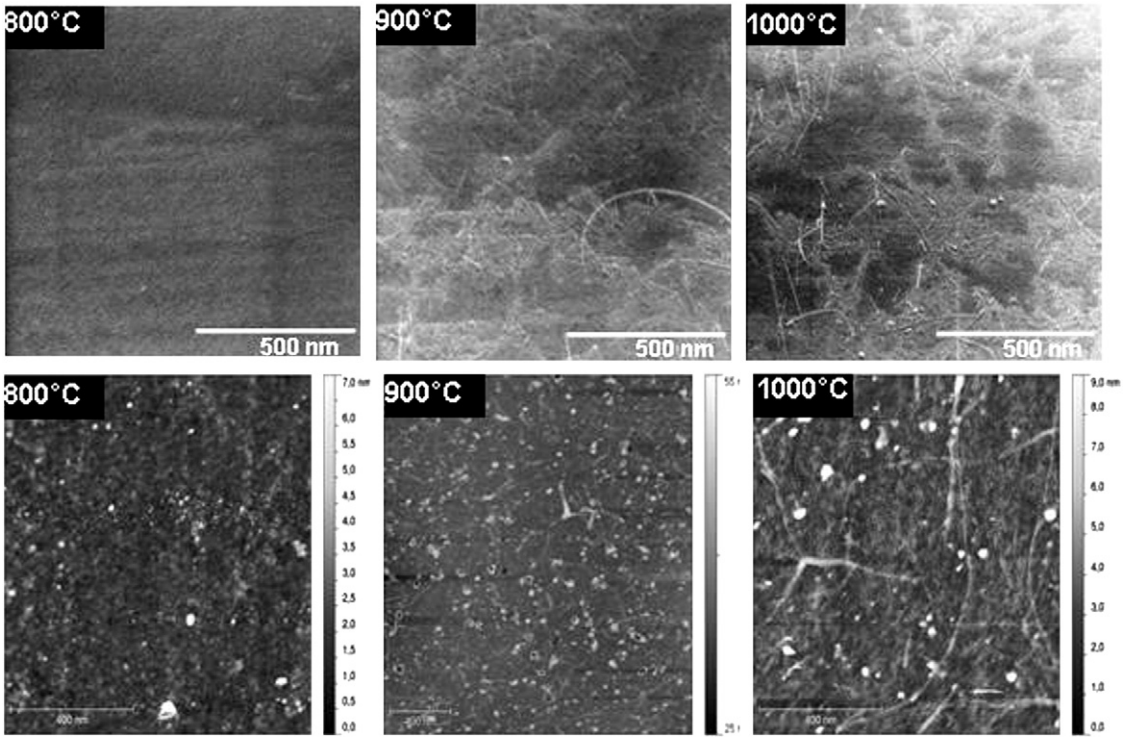

Fig. 4. SEM and AFM micrographs of SWCNTs deposited at different growth temperatures: 800 °C, 900 °C and 1000 °C.

carbon nanotubes were efficient at these temperatures. In addition the effect of the growth temperature on the CNTs diameter, we can also notice another change of the CNTs morphology: when grown at 1000 °C they are more straight and better aligned than those grown at lower temperatures (Fig. 4). These results are consistent with the previously reported results [34].

4. Conclusion

This work presents the synthesis of single walled carbon nanotube on Ru catalyst via hot filament assisted chemical vapor deposition (HFCVD). Self assembled monolayers of Ru tetraphenyl porphyrins (RuTPP) were used as catalyst on the SiO_2/Si(100) growth substrates pre-functionalized by silanisation to form a pyridine terminated molecular monolayer. SWCNTs could be synthesized by HFCVD on such catalyst surfaces with excellent selectivity and high quality. The experimental results indicate a significant influence of hot filament and the growth temperature on the diameter and the crystallinity of the SWCNTs. It was found that a higher density of longer SWCNTs is obtained with the hot filament assistance, while the SWCNTs diameter increases with increasing the growth temperature.

References

[1] M.S. Dresselhaus, G. Dresselhaus, P. Avouris (Eds.), Carbon Nanotubes Synthesis, Structure, Properties, and Applications, Springer, Berlin, 2001.
[2] A. Loiseau, P. Gadelle, P. Peigney, X. Blase, J.C. Charlier, M. Ducastelle, Growth mechanism of carbon nanotubes, in: Loiseau, et al., (Eds.), Understanding Carbon Nanotubes: From Theory to Applications, Springer, Berlin, 2006, p. 49.
[3] Y.M. Lin, J. Appenzeller, J. Knoch, P. Avouris, IEEE Trans. Nanotechnol. 4 (2005) 481.
[4] Y. Hayamizu, T. Yamada, K. Mizuno, R.C. Davis, D.N. Futaba, M. Yumura, K. Hata, Nat. Nanotechnol. 3 (2008) 289.
[5] V. Lovat, D. Pantarotto, L. Lagostena, B. Cacciari, M. Grandolfo, M. Righi, G. Spalluto, M. Prato, L. Ballerini, Nano Lett. 5 (6) (2005) 1107.
[6] H. Dai, J.H. Hafner, A.G. Rinzler, D.T. Colbert, R.E. Smalley, Nature 384 (1996) 147.
[7] S. Chaisitsak, A. Yamada, M. Konagai, Diamond Relat. Mater. 13 (2004) 438.
[8] A.C. Dillon, A.H. Mahan, J.L. Alleman, M.J. Heben, P.A. Parilla, K.M. Jones, Thin Solid Films 430 (2003) 292.
[9] V.I. Merkulov, A.V. Melechko, M.A. Guillorn, D.H. Lowndes, M.L. Simpson, Appl. Phys. Lett. 79 (2001) 2970.
[10] C.S. Cojocaru, F. Le Normand, Thin Solid Films 515 (2006) 53.
[11] D.B. Hash, M. Meyyappan, J. Appl. Phys. 93 (2003) 750.
[12] A.H. Jayatissa, K. Guo, Vacuum 83 (2009) 852.
[13] V. Huc, F. Armand, J.P. Bourgoin, S. Palacin, Langmuir 17 (6) (2001) 1928.
[14] V. Huc, M. Saveyroux, J.P. Bourgoin, F. Valin, G. Zalczer, P.A. Albouy, S. Palacin, Langmuir 16 (4) (2000) 1770.
[15] W. Kern, Semicond. Int. (1984) 94.
[16] F. Bouanis, L. Baraton, C. Sorin-Cojocaru, V. Huc, in preparation.
[17] F. Armand, P.A. Albouy, F.D. Cruz, M. Normand, V. Huc, E. Goron, Langmuir 17 (11) (2001) 3431.
[18] H.J. Jeong, L. Eude, M. Gowtham, B. Marquardt, S.H. Lim, S. Enouz, C.S. Cojocaru, Y.H. Lee, D. Pribat, Nano 3 (3) (2008) 145.
[19] R.S. Tsang, P.W. May, M.N.R. Ashfold, K.N. Rosser, C.A. Rego, Diamond Relat. Mater. 6 (1997) 247.
[20] P.W. May, Y.A. Mankelevich, J. Appl. Phys. 100 (2006) 024301.
[21] M.S. Dresselhaus, G. Dresselhaus, A. Jorio, A.G. Souza Filho, R. Saito, Carbon 40 (2002) 2043.
[22] P.C. Eklund, J.M. Holden, R.A. Jishi, J. Carbon 33 (7) (1995) 959.
[23] W.Z. Li, H. Zhang, C.Y. Wang, Y. Zhang, L.W. Xu, K. Zhu, S.S. Xie, J. Appl. Phys. Lett. 70 (20) (1997) 2684.
[24] V. Georgakilas, D. Gournis, M.A. Karakassides, D. Petridis, J. Carbon 42 (4) (2004) 865.
[25] R. Kamalakaran, M. Terrones, T. Seeger, P. Kohler-Redlich, M. Ruhle, Y.A. Kim, T. Hayashi, M. Endo, Appl. Phys. Lett. 77 (21) (2000) 3385.
[26] A.M. Rao, E. Richter, S. Bandow, B. Chase, P.C. Eklund, K.A. Williams, S. Fang, K.R. Subbaswamy, M. Menon, A. Thess, R.E. Smalley, G. Dresselhaus, M.S. Dresselhaus, Science 275 (1997) 187.
[27] A. Jorio, R. Saito, J.H. Hafner, C.M. Lieber, M. Hunter, T. McClure, G. Dresselhaus, M.S. Dresselhaus, Phys. Rev. Lett. 86 (2001) 1118.
[28] Y. Murakami, E. Einarsson, T. Edamura, S. Maruyama, Carbon 43 (2005) 2664.
[29] A. Jorio, R. Saito, J.H. Hafner, C.M. Lieber, M. Hunter, T. McClure, G. Dresselhaus, M.S. Dresselhaus, Phys. Rev. Lett. 86 (6) (2001) 1118.
[30] S.M. Guláš, C.S. Cojocaru, F. Le Normand, S. Farhat, Plasma Chem. Plasma Process. 28 (2008) 123.
[31] C. Singh, M.S.P. Shaffer, A.H. Windle, Carbon 41 (2003) 359.
[32] H. Zhang, E. Liang, P. Ding, M. Chao, Physica B 337 (2003) 10.
[33] A.H. Jayatissa, K. Guo, Vacuum 83 (2009) 853.
[34] X.H. Chen, R.M. Wang, J. Xu, D.P. Yu, Micron 35 (2004) 455.